ACS central science

http://pubs.acs.org/journal/acscii

Research Article

Bridging Hydrometallurgy and Biochemistry: A Protein-Based Process for Recovery and Separation of Rare Earth Elements

Ziye Dong, Joseph A. Mattocks, Gauthier J.-P. Deblonde, Dehong Hu, Yongqin Jiao, Joseph A. Cotruvo, Jr.,* and Dan M. Park*

Cite This: *ACS Cent. Sci.* 2021, 7, 1798−1808

Read Online

ACCESS | Metrics & More | Article Recommendations | Supporting Information

ABSTRACT: The extraction and subsequent separation of individual rare earth elements (REEs) from REE-bearing feedstocks represent a challenging yet essential task for the growth and sustainability of renewable energy technologies. As an important step toward overcoming the technical and environmental limitations of current REE processing methods, we demonstrate a biobased, all-aqueous REE extraction and separation scheme using the REE-selective lanmodulin protein. Lanmodulin was conjugated onto porous support materials using thiol-maleimide chemistry to enable tandem REE purification and separation under flow-through conditions. Immobilized lanmodulin maintains the attractive properties of the soluble protein, including remarkable REE selectivity, the ability to bind REEs at low pH, and high stability over numerous low-pH adsorption/desorption cycles. We further demonstrate the ability of immobilized lanmodulin to achieve high-purity separation of the clean-energy-critical REE pair Nd/Dy and to transform a low-grade leachate (0.043 mol % REEs) into separate heavy and light REE fractions (88 mol % purity of total REEs) in a single column run while using ∼90% of the column capacity. This ability to achieve, for the first time, tandem extraction and grouped separation of REEs from very complex aqueous feedstock solutions without requiring organic solvents establishes this lanmodulin-based approach as an important advance for sustainable hydrometallurgy.

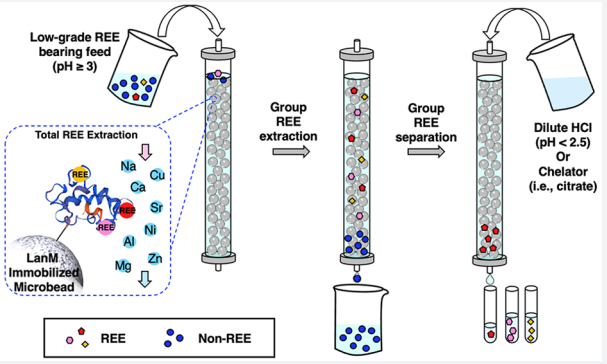

INTRODUCTION

Rare earth elements (REEs), comprising the lanthanides, yttrium, and scandium, are essential for the transition from the fossil fuel era into the low-carbon era.[1] Five REEs (Tb, Dy, Eu, Nd, and Y) in particular have been highlighted by the U.S. Department of Energy for supply vulnerability and criticality for clean energy technologies, such as electric vehicles, wind turbines, and LEDs.[2] Conversely, however, current REE extraction and separation processes require high energy consumption and pose severe environmental burdens that impede the development of a diversified REE supply chain and undercut the environmental benefits of clean energy technologies.[3,4] To meet the REE demands of the emerging clean energy technology market, it is thus imperative to develop new processing methodologies that enable environmentally friendly REE extraction from current and future resources.

Owing to their similar chemical properties and co-occurrence in REE-bearing deposits,[5,6] the separation among REEs is particularly difficult, accounting for ∼30% of the total environmental impact during REE production.[3,7,8] Currently, REE separation is dominated by organic solvent-intensive hydrometallurgy processes that involve a primary REE separation from impurities in acid leachate solutions and subsequent group or individual REE separation by liquid−liquid extraction.[6] In order to achieve high-purity single REEs, liquid−liquid extraction may require hundreds of stages (i.e., mixer-settlers or pulsed columns), which requires a large process footprint and high investment cost and generates a large volume of secondary liquid waste. Furthermore, for environmental and economic reasons, liquid−liquid extraction is typically not directly compatible with dilute REE leachate solutions (REEs < 1%) from unconventional sources, such as industrial wastes (e.g., coal fly ash, mine tailings) and end-of-life consumer electronics (e.g., electronic waste, or "E-waste"), given the challenge of REE preconcentration from these sources relative to high-grade ores. In addition, such dilute leachate solutions require a higher aqueous to organic phase ratio, resulting in large separation units (i.e., high capital expenditure), longer equilibration time, higher energy cost, and losses of extractant dispersed into aqueous systems.[9] To reduce

Received: June 16, 2021
Published: October 8, 2021

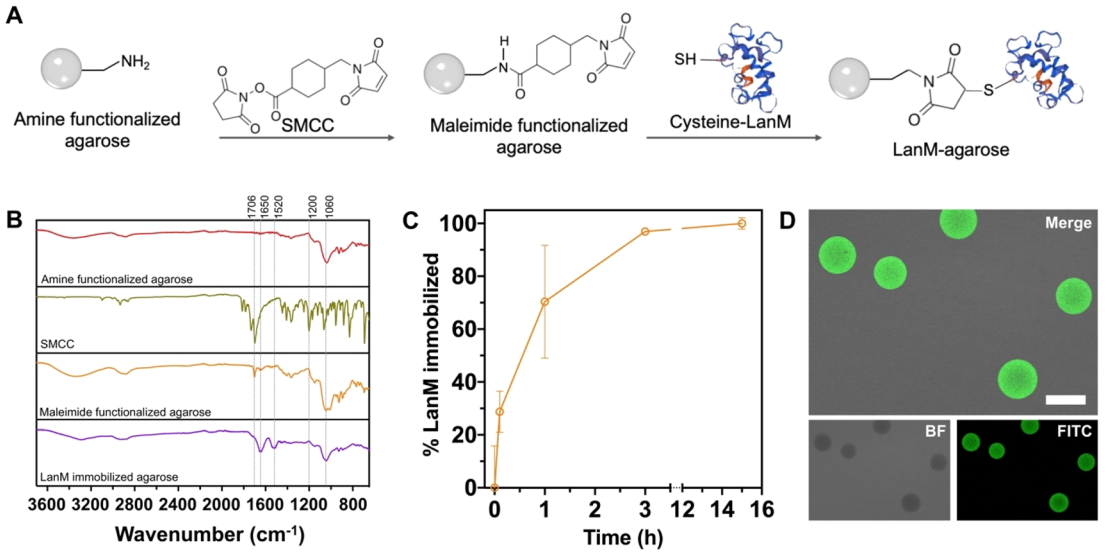

Figure 1. LanM immobilization and characterization. (A) Overall process for immobilization of LanM protein onto agarose microbeads through thiol-maleimide click chemistry. (B) Fourier transform infrared spectroscopy (FTIR) spectra of amino-agarose, *N*-succinimidyl 4-(maleimidomethyl) cyclohexane-1-carboxylate (SMCC), maleimide-agarose, and LanM-agarose (see the Supporting Information for further details of interpretation). (C) LanM immobilization kinetics, mean ± standard deviation for 3 independent measurements. (D) Fluorescence microscopy image confirming LanM immobilization onto agarose microbeads using FITC-LanM. Scale bar is 100 μm. Bottom images are split channels of the top image.

solvent losses, the liquid−liquid extraction process has been adapted for column chromatography by dissolving REE-selective ligands in organic solvent and loading within a solid support.[10−12] However, this physical impregnation strategy still inevitably results in leaching of the stationary liquid phase, causing cross-contamination and limited reusability.[13]

Ion exchange chromatography (IX) is an alternative to liquid−liquid extraction for intra-REE separation.[14] In conventional IX, REEs are separated based on differences in the metal ion migration rates in the presence of a chelating eluent [e.g., citrate or ethylenediaminetetraacetic acid (EDTA)] or by using a selective stationary phase (e.g., iminodiacetic acid-bound silica). IX approaches can achieve ultrapure (99.9999%) individual REEs in a single run with high yield[15] but are typically restricted to applications where small quantities of ultra-high-purity REEs are required (e.g., electronics or analytical applications) given the high cost and low productivity.[15] However, recent advances in process simulations and design methods have facilitated IX methods with higher productivity.[16] For example, a two-zone ligand-assisted displacement approach separated a ternary REE mixture (Pr, Nd, and Dy with a composition typical of magnet waste) into individual components (∼99%) at a production scale that is competitive with solvent extraction.[17] Nevertheless, the application of IX for intra-REE separation from feedstocks containing significant non-REE impurities remains a challenge considering the low REE selectivity of the resins.

Solid−liquid extraction, whereby chemical ligands with high REE affinity are covalently anchored onto solid support resin, provides an effective means to achieve REE recovery from complex feedstock leachates.[18,19] Here, REEs are selectively adsorbed to the resin until the column is saturated, at which point a stripping solution is applied to elute the REE concentrate. This process offers several advantages relative to liquid−liquid extraction,[18,20−22] including faster phase separation between the solid adsorbent and REE-bearing solution and high stability for reuse.[23] However, most of the solid-phase adsorbents employed for REE separation are based on existing chemical ligands, which limits the intra-REE separation potential of the process.[24]

The incorporation of biological ligands into a solid−liquid extraction process offers the potential for novel chemistries and environmentally sustainable REE separation process development.[25,26] For example, lanthanide binding tags (LBTs), short peptides that have been engineered for affinity and selectivity toward REEs, have been displayed on biomaterial surfaces (cells, curli fibers, etc.) and employed in solid−liquid extraction for selective recovery of middle and heavy REEs from various feedstock leachates.[27−29] However, the low selectivity against Cu^{2+} and negligible REE binding below a pH of 5 limit the feedstock compatibility of LBT.[27,30] More recently, the discovery of lanmodulin (LanM), a small (12 kDa) protein that is involved in lanthanide trafficking in methylotrophic bacteria, holds promise as a new ligand for process development.[31] Biochemical and biophysical characterization of LanM revealed remarkable selectivity for REEs against non-REE cations, the ability to bind REEs down to pH ≈ 2.5, and uncommon robustness (relative to other proteins) to repeated acid treatment cycles.[32] Despite the protein's high affinity, REE desorption can be induced by relatively mild treatments (lowering pH or common chelators like water-soluble carboxylates), allowing multiple cycles of binding and desorption. Furthermore, LanM also displayed an unusual preference toward middle−light REE over heavy REE; although modest [$K_{d(Dy)}/K_{d(Nd)} \sim 5$, ($K_d$ = dissociation constant)], such a preference might allow for efficient separation of light/heavy REE groups or even important REE pairs.[31]

Here, we report a bio-material-based, all-aqueous REE extraction and separation scheme using the REE-selective LanM protein chelator. To enable facile protein reuse, we immobilized LanM onto porous agarose microbeads, which are biorenewable and commercially available.[33] The resulting biomaterial allowed effective grouped REE extraction from

https://doi.org/10.1021/acscentsci.1c00724
ACS Cent. Sci. 2021, 7, 1798−1808

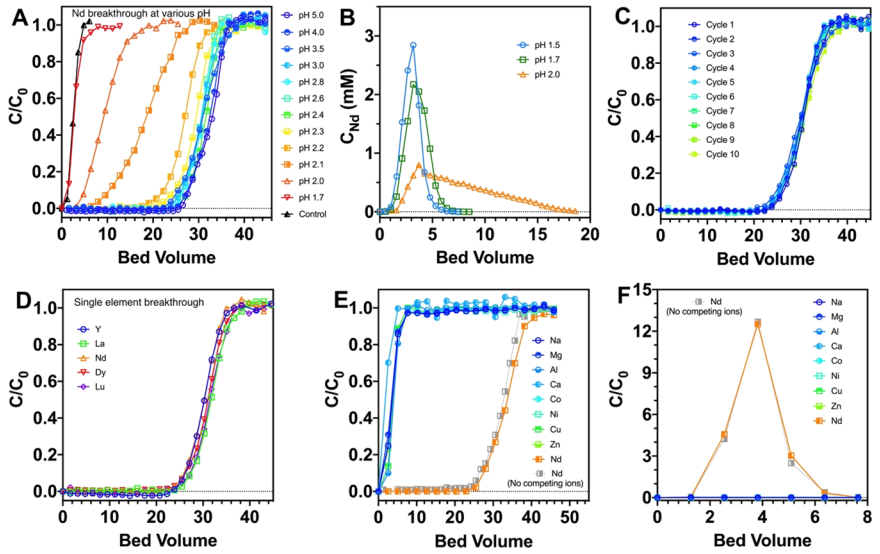

Figure 2. Immobilized LanM enables high-selectivity REE extraction at low pH. (A) Effect of pH on Nd breakthrough. Experimental conditions: 0.2 mM Nd in 10 mM glycine buffer (pH > 2.2 condition; for pH < 2.1 conditions, Nd was diluted in HCl solution), 0.5 mL/min flow rate. The control experiment was performed at pH 3 by using a column packed with maleimide-functionalized agarose. (B) Effect of HCl concentration on Nd desorption. Columns were preadsorbed with 40 bed volumes of 0.2 mM Nd at pH 3. (C) Column reusability shown by 0.2 mM Nd breakthrough curves for 10 consecutive adsorption/desorption cycles at a flow rate of 0.5 mL/min. Desorption condition: 10 bed volumes of pH 1.5 HCl. (D) Independent single-element breakthrough curves of Y, La, Nd, Dy, and Lu at pH 3. Feed: 0.2 mM. (E) Nd selectivity of the LanM column against non-REEs. Metal ion breakthrough curves using synthetic feed solution containing 0.2 mM Nd and order-of-magnitude higher concentrations of each non-REE at pH 3 (the detailed feed composition and uncertainties are listed in Table S1). (F) Desorption profile of metal ions following treatment with pH 1.5 HCl. For panels A–D, 1 bed volume = 0.94 mL. For panels E and F, 1 bed volume = 0.80 mL.

unconventional, low-grade REE feedstocks. Furthermore, by exploiting the preference of LanM for middle–light REE, we demonstrate proof-of-concept high-purity separation between REE pairs (Nd/Dy, and Y/Nd) and grouped separation between heavy REEs (HREE, Tb–Lu + Y) and light REEs (LREE, La–Gd). As such, a key advantage of this approach over liquid–liquid extraction is the combination of primary REE extraction from non-REEs and secondary separation between heavy and light REEs within a single, all-aqueous adsorption/desorption cycle. This advance greatly simplifies further processing and provides the basis for a full protein-based scheme for efficient REE extraction, concentration, and separation from both high- and low-grade feeds.

RESULTS AND DISCUSSION

Immobilization of LanM onto Agarose Microbeads. To facilitate the application of LanM for REE recovery in a flow-through format, we immobilized a LanM variant containing a C-terminal cysteine residue with a GSG spacer (hereafter LanM) on agarose microbeads using thiol-maleimide click chemistry (Figure 1A).[34,35] Compared with other immobilization strategies, such as physical binding and entrapment, site-specific covalent attachment enables a stable and surface-accessible protein display, which is desirable for repeated cycles of adsorption/desorption under harsh conditions (e.g., low pH and high ionic strength). Thiol-maleimide chemistry was pursued given the ease of encoding a terminal cysteine residue and the linkage's stability at low pH (*vide infra*). This construct exhibited REE binding consistent with the wild-type protein (Figure S1). Purified LanM was handled at low pH (see the Methods section in the SI) to preclude oxidation while avoiding the need for a reducing agent, which we found to adversely affect LanM immobilization (data not shown). Maleimide and LanM functionalization of the agarose beads was confirmed by FT-IR (Figure 1B; Supporting Information), and the immobilization kinetics were monitored by quantifying the free LanM concentration in the conjugation solution over a 16 h conjugation reaction. Approximately 97% of the added LanM was loaded within 3 h (Figure 1C), resulting in an immobilization density of 2.47 ± 0.54 μmol LanM/mL agarose. To visualize the distribution of LanM within the agarose bead, a fluorescently tagged variant of LanM (FITC-LanM, green) was incorporated during immobilization. Confocal microscopy imaging confirmed a homogeneous distribution of FITC-LanM within the agarose microbeads (Figure 1D).

Immobilized LanM Retains the Ability to Bind REEs at Low pH and Is Stable for Reuse. To test the efficacy of the immobilized LanM for REE extraction under flow-through conditions, fixed-bed columns were packed with the LanM conjugates, and influent breakthrough behavior was assessed with synthetic REE-containing solutions. Nd^{3+} was selected as a representative model REE due to its abundance in REE deposits and high criticality for renewable energy technologies.[2] The Nd breakthrough point (at pH 5) occurred after ~25 bed volumes, in contrast to 1 bed volume with nonconjugated agarose beads, which is due to the passage of the void volume, indicating that LanM retains high affinity for REEs upon immobilization (Figure 2A). The adsorption capacity of the LanM column was 5.77 ± 0.67 μmol/mL, which corresponds to a ~2:1 stoichiometry of Nd per immobilized LanM. Interestingly, in solution, LanM binds 3 equiv of REEs (Figure S1), suggesting that one metal site is destabilized or inaccessible upon immobilization, or in the column format. We suggest that this observation reflects the greater lability of metal ions bound to EF hand 1, especially at pH ≤ 5,[36] which may lead this site to not be stably occupied under flow-through conditions. The lability of EF hand 1 may

https://doi.org/10.1021/acscentsci.1c00724
ACS Cent. Sci. 2021, 7, 1798–1808

also explain the requirement that LanM be added at a 1:2 (REE:protein) rather than 1:3 stoichiometry to achieve quantitative REE extraction in prior experiments with industrial feedstock leachates.[32]

Given that our prior work revealed that solubilized LanM can bind REEs at a pH as low as 2.5−3, we tested the effect of influent pH on Nd extraction performance over the pH range 1.7−5 (Figure 2A). Our results indicate that immobilized LanM can effectively bind Nd down to pH 2.4, consistent with the results for solubilized LanM.[32] Nd binding to immobilized LanM is reduced by 50% at pH 2.2 and becomes insignificant at pH $\leq$ 1.7.

Taking advantage of the pH dependence of REE binding, we tested Nd desorption by pumping HCl solutions through Nd-saturated columns. A sharp desorption peak was observed between 1 and 6 bed volumes with pH $\leq$ 1.7 with Nd concentrated by over an order of magnitude relative to the feed solution (Figure 2B). In contrast, a pH 2.0 HCl solution yielded a tailed desorption profile with 16.5 bed volumes required to desorb >95% of the Nd. Importantly, the LanM-based sorbent was resilient to repeated low pH exposures given that 10 consecutive absorption/desorption cycles (pH 3.0 and 1.5, respectively) yielded no reduction in adsorption capacity (Figure 2C). To confirm the generalizability of low-pH binding, breakthrough curves with other representative REEs (i.e., Y, La, Dy, and Lu; Figure 2D) were performed at pH 3.0 and yielded indistinguishable results from that of Nd. Overall, the results demonstrate effective and reversible REE binding by immobilized LanM under low-pH conditions.

LanM Enables High-Purity Recovery and Concentration of REEs. To test the REE selectivity of immobilized LanM, Nd (0.2 mM) breakthrough experiments were conducted with a synthetic feed solution at pH 3.0 that contained millimolar concentrations of Mg^{2+}, Al^{3+}, Ca^{2+}, Co^{2+}, Ni^{2+}, Cu^{2+}, and Zn^{2+}, which are abundant in REE-containing feedstocks.[15] The breakthrough of Nd occurred after 24 bed volumes (Figure 2E), whereas all non-REEs emerged with the void volume. Importantly, the Nd breakthrough curve and subsequent desorption curve were indistinguishable from the curves observed with a synthetic solution lacking non-REEs (Figure 2E,F), indicating that the behaviors of the REE and non-REE are completely decoupled in the process owing to the selectivity of LanM. Lastly, whereas the limited solubility of Fe^{3+} precluded its use in the multielement experiment, a breakthrough experiment using a binary Nd/Fe solution containing citrate to maintain Fe solubility through coordination confirmed the selectivity of LanM for Nd^{3+} over Fe^{3+}(Figure S2 and Table S2). Collectively, these results show that immobilized LanM retains the high REE selectivity of LanM in solution and can be employed to separate REEs from non-REEs.

Ligand Competition with Nonimmobilized LanM Reveals Potential for Intra-REE Separations. LanM exhibits an inverse affinity trend relative to most REE ligands (e.g., diglycolamides[37]) with a preferential response to LREEs.[38] However, despite our studies of REE extraction in solution[32] and on column (*vide supra*), we had not yet attempted to exploit these affinity differences for intra-REE separations (*vide infra*). We reasoned that competition with a mild chelator with a preference for HREEs, such as citrate,[39] could allow for enhanced selectivity in a desorptive process. To establish this principle, we first investigated ligand competition with nonimmobilized LanM. We took advantage of our observation that the fluorescence of the sole tyrosine residue in LanM (Y96), which is adjacent to EF hands 2 and 3, is quenched upon REE binding, which may reflect differences in solvent exposure and hydrogen bonding.[31] Titrations of LanM with REE displayed a maximal change in tyrosine fluorescence at 2 equiv of REE, which was counteracted upon binding of the third equivalent (Figure 3A). Our recent work has identified

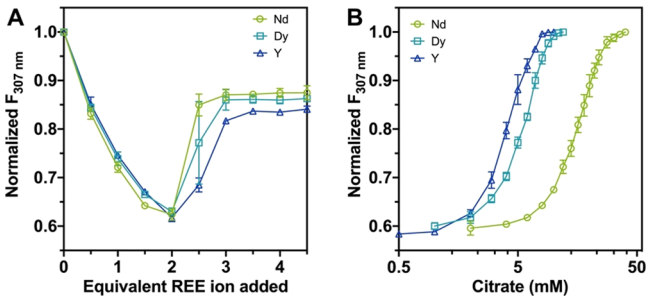

Figure 3. Spectrofluorometric titrations of LanM. (A) Fluorometric titration of LanM (20 μM) with Nd^{3+}, Dy^{3+}, and Y^{3+}, showing quenching of tyrosine fluorescence upon metal binding. (B) Desorption of LanM bound to 2 equiv of each metal using citrate, followed fluorometrically. Excitation at 278 nm, emission at 307 nm, pH 5.0. All data points represent mean ± standard deviation for 3 independent experiments.

EF1 as the weakest of LanM's three lanthanide binding sites; therefore, we suggest that the first two equivalents of metal bind to EF2/3, and the third equivalent (to EF1) perturbs the environment of Y96.[36] This fluorescence change provides a convenient handle with which to assay conditions for REE desorption from LanM. These studies, using titrations with LanM bound to individual REEs, revealed that citrate selectively outcompeted LanM for HREEs before LREEs, as expected given LanM's apparent K_d's (Figure 3B). For example, 10 mM citrate is sufficient to fully desorb Dy from LanM, whereas Nd is still mostly bound to the protein. The sharp desorption profiles (occurring over a 4-fold concentration range) are consistent with cooperativity in LanM's metal binding.[31] These results demonstrate that, despite LanM's high REE affinity, mild chelators can be used to desorb REEs. Furthermore, and importantly, an adjustment of conditions can be used to selectively desorb HREEs from LanM without destabilizing LREE-LanM complexes, setting the stage for on-column separations.

On-Column Separation between REE Pairs. Next, we examined whether judicious selection of desorption conditions could allow on-column separation among REEs, first using individual REE-loaded LanM columns over a range of pH (Figure 4A) and citrate steps (Figure S3A). A representative set of REEs (Y, La, Pr, Nd, Dy, and Lu) was tested independently to cover the entire ionic radius range of lanthanides (La and Lu) and based on their criticality for renewable energy technologies (Y, Pr, Nd, and Dy). Distinct elution profiles were observed for each REE using both desorption options (Figure 4A and Figure S3A). For citrate, the order of REE elution was correlated with the ionic radius and closely matched the solution data (Figure 3). A similar trend was observed for pH, with the notable exception that Nd required a lower pH for desorption compared to La. This result is suggestive of higher relative stability for the LanM-Nd complex compared to LanM-La and is consistent with a local maximum in stability for LanM in the Nd/Pr range.[31,32] We

https://doi.org/10.1021/acscentsci.1c00724
ACS Cent. Sci. 2021, 7, 1798−1808

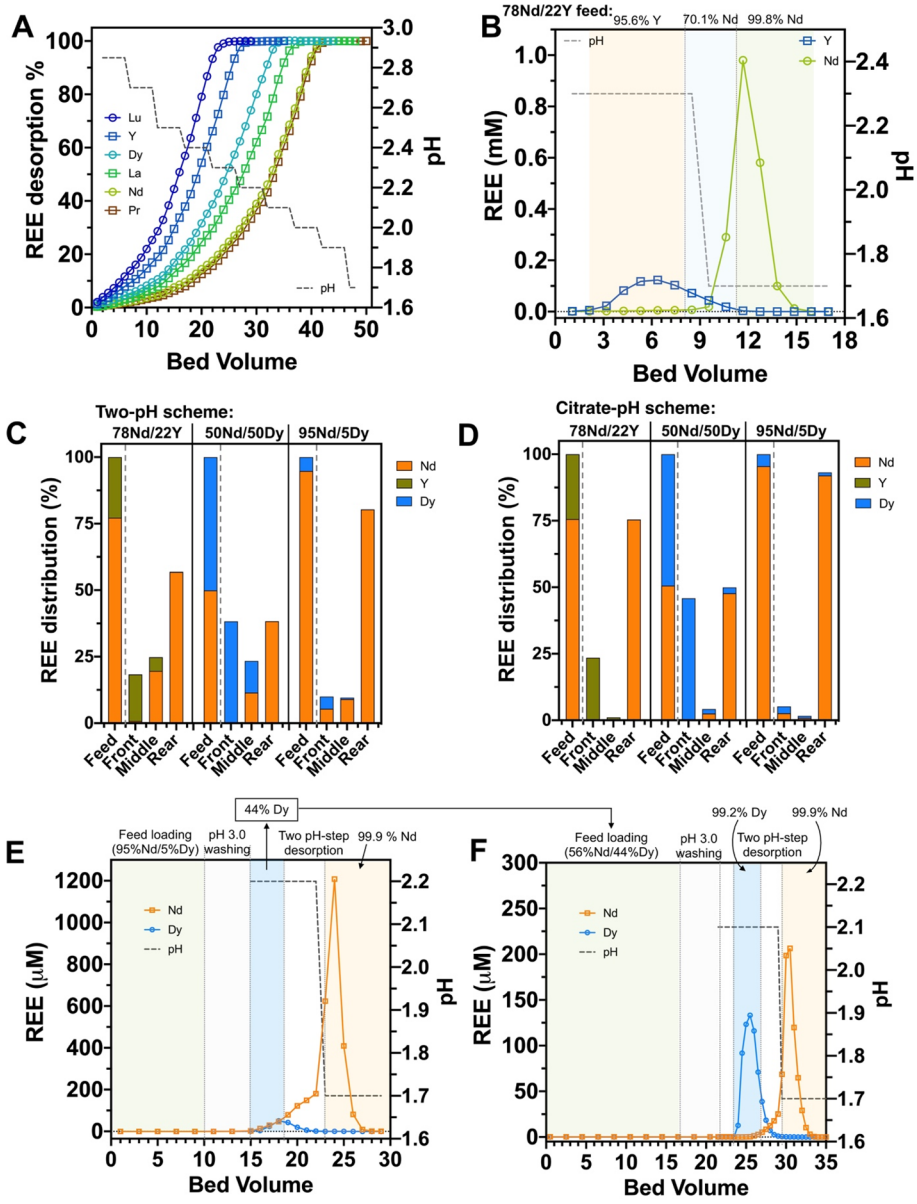

Figure 4. LanM enables high-purity separation of Nd/Y and Nd/Dy pairs. (A) Accumulative desorption profiles of single-element independently loaded columns using a stepwise pH scheme. REE ion desorption was normalized to the total REE desorbed. (B) Two-pH desorption scheme of a binary REE-loaded column. Experimental conditions: REE solutions (Nd:Y = 78:22) at pH 3 were used to load the column to 75% saturation before a pH 2.3 and pH 1.7 desorption step was carried out (feed loading and washing not shown). The values above each panel indicate the purity of REE over each elution zone. The duration of each pH step is depicted by the dark gray dashed line. Summary of the REE distribution in the initial feedstock and three desorption regions relative to the total REE in feed solution using (C) a two-pH scheme and (D) citrate-pH scheme, respectively. (E, F) Demonstration of Dy/Nd separation using two coupled adsorption/desorption cycles. (E) A feedstock comprising a 5:95 mixture of Dy:Nd was subjected to a two-step pH desorption scheme that was repeated 5 times (Figure S4C). The resulting Dy-rich desorption fractions were combined, adjusted to pH 3 by adding concentrated glycine buffer (1 M), and used as a feed solution in a second adsorption/desorption cycle. (F) Two-step pH desorption scheme with the combined 44% Dy/56% Nd solution. The zones of feed loading, washing, and each desorption step are divided by vertical dotted gray lines. The detailed feed composition and measurement uncertainties are listed in Tables S3 and S5. For panels A and B, 1 bed volume = 0.94 mL. For panels E and F, 1 bed volume = 1.0 mL.

anticipated that the differences in stability among tested LanM REE complexes could be exploited to achieve separation between certain REE pairs.

Guided by the above results, we first tested the ability of LanM to separate Y from Nd (Figure 4B and Figure S3B), as both REEs are abundant in primary REE deposits (e.g., those bearing monazite, xenotime, and/or allanite) and coal byproducts.[6,32] The proportion of Y and Nd in the feed solution was set to 22% and 78%, respectively, to resemble the HREE and LREE compositions in typical coal byproduct leachates.[40,41] The LanM column was loaded to ∼75% saturation (∼1 bed volume before breakthrough point, C/C_0 = 0.05) followed by either a two-pH desorption scheme or by combining an initial citrate-mediated Y desorption followed by pH-mediated elution of Nd. Two distinct peaks were collected after the two-step pH desorption, with 95.6% Y purity and 99.8% Nd purity achieved, respectively (Figure 4C). A small overlap region (<25% of the adsorbed metals) of nearly

https://doi.org/10.1021/acscentsci.1c00724
ACS Cent. Sci. 2021, 7, 1798−1808

identical composition as the influent feed solution (20.9% Y + 79.1% Nd) was collected and can be recycled as feed solution in a subsequent adsorption/desorption cycle. Remarkably, desorption using 15 mM citrate eluted 95.8% of the adsorbed Y at 99.4% purity, while a subsequent pH desorption step eluted 99.7% of the Nd at >99.9% purity (Figure 4D). Thus, with a single adsorption/desorption cycle with the LanM-based column, Y can be separated from Nd, supporting the feasibility of a HREE vs LREE separation step.

We next tested the efficacy of the LanM column to separate the clean-energy-critical REE pair Dy/Nd by loading the column to ∼75% saturation with a solution of Nd and Dy at a 50:50 molar ratio followed by a stepwise desorption process (Figures S4A and S3C). For the two-pH scheme, 76.2% of the Dy was eluted with 99.9% purity with an initial pH 2.1 desorption, while 76.8% of the Nd was eluted with 99.9% purity with a second pH 1.7 desorption. Notably, both products exceed the minimal purity threshold (99.5% rare earth oxide) for salability.[42] Less than 24% of the loaded REE material was present in the peak overlap region; considering the identical Nd/Dy composition as the feed solution (50.8% Dy; Figure S4A), this fraction can be combined with the initial feed solution and processed during a future purification cycle (hence, avoiding any loss of REE). The citrate/pH combination eluted 94.2% of the adsorbed Dy at a purity of 99.1%, while a subsequent pH desorption step eluted the remaining Nd (99.2%) at a purity of 94.6% (Figure S3C). Collectively, these results show that the LanM column can produce high-purity Dy/Nd products when starting with an equimolar mixture of both metal ions.

To test with a feedstock composition that reflects NdFeB magnet-bearing E-waste, we loaded the column to ∼75% saturation with a feed solution comprising 95% Nd and 5% Dy.[43] The use of Nd as a surrogate for the combined Nd/Pr content (typically 3:1 Nd:Pr) is supported by the nearly identical desorption profiles of both metal ions as a function of pH or citrate concentration (Figure 4A and Figure S3A). Successful separation of Dy from Nd/Pr would enable the production of high-value dysprosium and didymium (NdPr) oxide products that could be fed back into the magnet manufacturing supply chain. As shown in Figures S4B and S3D, both the two-pH and citrate desorption schemes yielded high-purity Nd fractions (99.8% and 98.7%, respectively) while significantly upgrading the Dy purity. For example, a pH 2.2 elution step yielded 88.6% of the Dy content at 46.1% purity while the citrate desorption step yielded 73.9% of the Dy at a purity of 50.3%. Given the earlier results with 50:50 mixtures, we hypothesized that the roughly 50% purity Dy fractions can be further upgraded to high purity by using a second adsorption/desorption cycle. To confirm this hypothesis, we repeated the Nd/Dy separation using the 95% Nd/5% Dy feed 5 times to accumulate a sufficient volume of a 44% purity Dy desorption fraction to enable a second separation step (Figure 4E and Figure S4C). Despite the dilute nature of the Nd/Dy feed solution, the LanM column exhibited a high loading yield (>99%) and achieved 88% of Dy at a purity of 99.2% and 82% of Nd at a purity of 99.9%, respectively, following the pH desorption step. Our results suggest that the LanM column is able to effectively separate Dy from Nd starting with low-purity Dy solutions typical of E-waste leachates. We anticipate that an even higher yield and product purity will be achieved with higher operational volumes. In addition, further REE separations can likely be realized upon the fine-tuning of column operation conditions, such as pH, competing chelator identity and concentration, flow rate, and column geometry. Such optimization will be the subject of future studies.

To facilitate a comparison of our LanM-based separation approach with the prior art, we present the feed composition, operating conditions, and product purity achieved in several exemplary REE separation studies in Table S4. When compared to liquid−liquid extraction and novel crystallization-based approaches, LanM enables a comparable Nd/Dy separation efficacy in an equal or fewer number of steps without using organic solvent (Table S4). For example, a liquid−liquid extraction process using bis(2,4,4-trimethylpentyl) phosphinic acid (Cyanex 272) in kerosene for Nd/Dy separation concentrated a feed solution containing 6.7% Dy to ∼47% purity Dy using a single extraction stage with 92.3% Dy extraction yield.[44] Similarly, a counter-current extraction configuration with 2-ethylhexyl phosphonic acid mono-2-ethylhexyl ester (PC88A) extractant in kerosene required three extraction stages to upgrade a 16% Dy/84% Nd feed solution to a 74.5% purity Dy solution, while a fourth extraction stage only increased the Dy purity to 94.6%.[45] Additionally, novel tripodal ligands have been used to separate 50:50 and 25:75 Dy:Nd solutions into 95% purity products by leveraging differences in the solubility of the resulting Dy/Nd complexes in organic solvent (i.e., tetrahydrofuran, benzene, or toluene).[46,47] As such, our results suggest that immobilized LanM can be used as an effective and environmentally friendly alternative to organic solvent-based extraction processes for the production of high-purity (up to 99.9%) Nd and Dy.

Despite being column-based, these stepwise desorption schemes using immobilized LanM are fundamentally different from traditional ion exchange chromatography.[48,49] In our experiments, ∼75% LanM column capacity was utilized in a single adsorption/stepwise desorption cycle, whereas only a small volume of feed solution (∼2−5% with respect to column size) is processed in a typical chelation ion chromatography cycle, due to the requirement of repeatedly partitioning (adsorption/desorption) between the mobile and ligand-functionalized stationary phases, which yields higher-purity REEs but limits the throughput of the separation process.[49] As such, our approach exceeds the capacity of traditional ion exchange chromatography while still achieving a high-purity product. In contrast, the capacity of the LanM approach is lower, but purity is higher compared to the recently developed two-stage ligand-assisted displacement chromatography that effectively separated a ternary REE mixture (Pr, Nd, and Dy) into individual components at ∼99% purity.[17] However, it is unclear whether the ligand-assisted displacement process would be compatible with non-REE impurities present in the initial feed. Based on the results in Figure 2E, we hypothesized that LanM will select against such impurities in the adsorption step, thereby uniquely allowing the REE extraction and selective desorption steps to be coupled.

Grouped REE Extraction and Separation from a Low-Grade Feedstock Leachate. Recovering REEs from abundant waste products, such as coal fly ash and red mud, provides a potential means to diversify the REE supply while avoiding pollution inherent to mining. However, the leachate solutions produced from such low-grade REE-bearing wastes, which contain high levels of metal ion impurities, such as Al^{3+}, Ca^{2+}, and Fe^{3+}, are problematic for traditional liquid−liquid extraction approaches.[6,15] For example, Al^{3+} is commonly coextracted with REEs in liquid−liquid extraction, resulting in

https://doi.org/10.1021/acscentsci.1c00724
ACS Cent. Sci. 2021, 7, 1798−1808

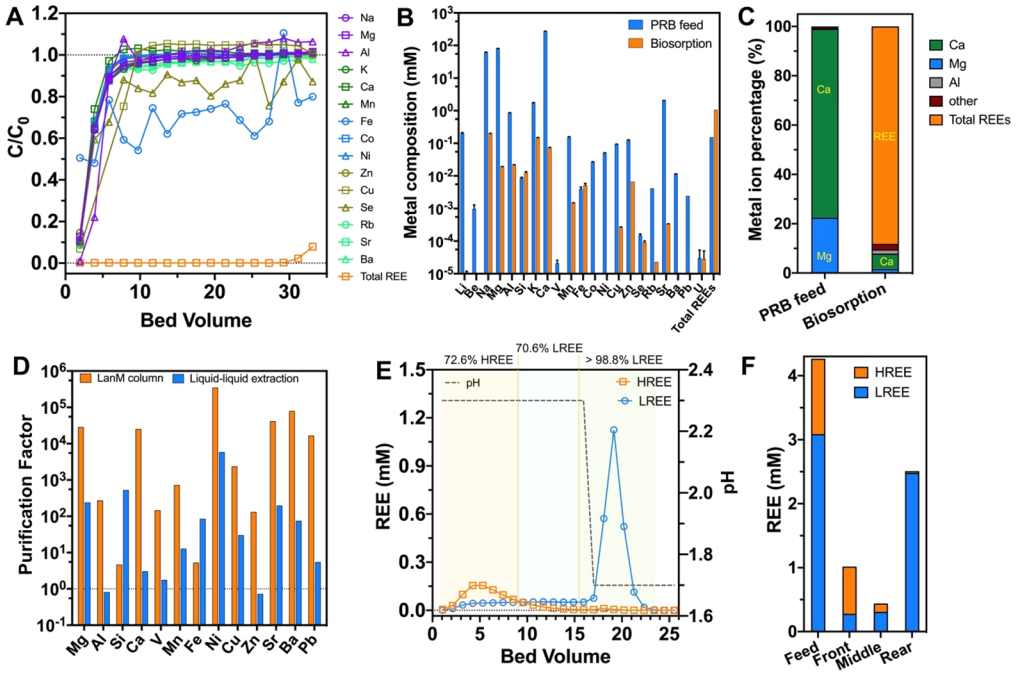

Figure 5. A LanM column facilitates REE recovery and grouped REE separation from a Powder River Basin (PRB) fly ash leachate solution. (A) Adsorption profiles of metal ions. Adsorption condition: pH 5, 0.5 mL/min. One bed volume = 0.8 mL. (B) Metal compositions in PRB feed and recovered biosorption solutions (desorption fractions 2–4 from Figure S5). Desorption was performed by using the column used in panel A after 35 bed volumes of adsorption. Note that, because the column adsorption was carried out slightly past the breakthrough point (30 bed volumes), some displacement of the heaviest REEs (Ho–Lu) by LREEs had occurred (see Table S6). (C) Metal ion percentage in PRB feed and recovered biosorption solutions (excluding monovalent ions). (D) Purification factor for total REEs relative to selected non-REEs. The values for liquid–liquid extraction were determined from the data of Smith et al.,[55] which used di-2-ethyl-hexylphosphoric acid (DEHPA) to extract REEs from fly ash generated from Appalachian coal using a single-stage liquid–liquid extraction with kerosene. Values above the dotted line indicate REE selectivity over non-REE. (E) Selective desorption of HREE (Tb–Lu, Y) and LREE (La–Gd) using a two-step pH scheme. The values above panel D indicate the purity of LREE or HREE versus total REE contents. Three elution zones are divided by vertical dotted lines. Experimental conditions: 29.1 bed volumes of PRB fly ash leachate was pumped through a 0.94 mL column, followed by a washing step with 10 bed volumes of pH 3.5 water. Desorption was performed with 16 bed volumes of pH 2.3 HCl solution and 10 bed volumes of pH 1.7 HCl solution, sequentially. (F) HREE and LREE distribution in the PRB feed and each elution zone feed from panel E relative to the total REE in PRB. The detailed ion composition and measurement uncertainty are listed in Tables S6–S8.

low REE purity and the formation of emulsions or a third phase via gelatinous hydroxides.[15] Similarly, other impurities, such as Ca^{2+}, may cause fouling in liquid–liquid extraction processes through gypsum formation.[50] As such, leachate solutions are commonly subjected to a pretreatment precipitation step to remove impurities before feeding into a liquid–liquid extraction unit. Although selective precipitation is effective for removing certain impurities, such as Fe^{3+}, the complete removal of Al^{3+} presents a major challenge as REE hydroxides coprecipitate with aluminum hydroxide.[15,51,52] Therefore, an REE extraction method with high REE selectivity over non-REE impurities, particularly Al^{3+} and Ca^{2+}, is highly desirable.

As an industrially relevant performance test, we demonstrated LanM column-based REE extraction and separation concepts using an exceptionally low-grade leachate (0.043 mol % REE, excluding monovalent ions) prepared from Powder River Basin (PRB), USA, fly ash.[53,54] The leachate contains ~150 μM total REEs compared with millimolar levels of Na, Mg, Al, Ca, and Sr (Table S6) and significant transition metal content (e.g., Zn, Ni, Cu, and Mn). Using the LanM-based column, the breakthrough of REEs occurred after 30 bed volumes, whereas non-REEs were eluted in the void volume (Figure 5A). To assess the REE purity of the adsorbed metal content, the metal ion composition was determined following nonselective desorption using a pH 1.5 solution. Over 96.5% of the REEs were desorbed within the most concentrated fractions (total 3.9 bed volumes, Figure 5B and Figure S5). A total REE purity of 88.2% was observed (Figure 5C), indicating a striking 2040-fold increase in purity compared with the feed solution (0.043 mol % REEs). Importantly, the radionuclide uranium was not concentrated from the PRB leachate.

To benchmark the REE selectivity of the LanM-based solid-phase adsorption with a liquid–liquid extraction approach (Figure 5D), the purification factor (see the Methods section in the SI for a definition) for total REEs relative to base metal ions was compared with data recently generated by Smith et al. using the commercial extractant di-2-ethyl-hexylphosphoric acid (DEHPA), with coal fly ash leachate of a comparable composition.[55] The LanM-based approach exhibited significantly higher selectivity against all non-REE impurities (purification factors of between 100 and 500 000 for the LanM column, depending on the element, versus only 10–5000 for the liquid–liquid extraction procedure) with the exception of Fe and Si. The high selectivity of LanM for REEs over Mg^{2+}, Al^{3+}, and Ca^{2+} is particularly compelling considering their abundance in low-grade feedstock leachates.[41,56] This improved selectivity represents a key advance over our prior biosorption-based REE extraction method using

https://doi.org/10.1021/acscentsci.1c00724
ACS Cent. Sci. 2021, 7, 1798–1808

LBT-displayed *Escherichia coli* cells, which was adversely affected by the high Ca/Mg content of the PRB leachate.[54] This selectivity advantage is expected to be even more pronounced at lower pH, where a higher solubility of metal ion impurities (e.g., Al) is observed. We suspect that the lower relative selectivity against Si and Fe reflects the formation of unfilterable colloid particles that accumulate on-column and are dissolved during the low-pH desorption step.[57] As such, our current column-based approach necessitates precolumn methods to minimize Fe/Si content to maximize the effect of LanM. In sum, these results highlight the ability of the immobilized LanM to selectively concentrate REEs from low-grade leachates containing a wide array of metal ion impurities.

Having demonstrated effective removal of the vast majority of non-REE impurities during the adsorption stage, we next tested the ability of LanM to achieve grouped separation of the REEs adsorbed from the PRB leachate [72% LREE (La−Gd); 28% HREE (Tb−Lu, Y)] using a two-pH desorption scheme. Grouped separation of REEs into HREE and LREE fractions is an important early step during liquid−liquid extraction and requires multiple extraction and stripping stages to enrich for HREEs, typically involving the use of a different extractant from that used in the non-REE removal stage.[6] In the case of the LanM-based column, two distinct peaks composed predominantly of either HREEs or LREEs were observed (Figure 5E); 82% of the HREEs were eluted with 72.6% purity at pH 2.3, while 80% of the LREEs were eluted with 98.8% purity at pH 1.7 desorption. Importantly, such group separation was achieved with ∼90% REE loading (29.1 bed volumes). We anticipate that even higher-purity LREE and HREE fractions could be achieved with lower REE loading. In previously proposed methods, to achieve a similar-purity LREE separation from an acid leachate generated from ion adsorption ores, 11 stages of counter-current extraction through a stepwise liquid−liquid extraction process involving the sequential use of 2-ethyl-hexyl phosphonic acid mono-2-ethylhexyl ester (HEH(EHP), P507) and di(2-ethylhexyl)phosphoric acid (HDEHP, P204) were required.[58] Collectively, these results highlight an unprecedented advantage of the LanM column: the ability to achieve both non-REE impurity removal and grouped REE separation starting from low-grade leachates in a single adsorption/desorption step without using organic solvent or hazardous chemicals. Based on our separation data with Nd/Dy, and Nd/Y pairs, we anticipate that finer separation within the HREE and LREE groups is possible by linking a small number of adsorption/desorption steps and/or by judicious incorporation of water-soluble chelators in the desorption step.

The applicability of this LanM-based biosorption technology for industrial-scale REE extraction and separation will require scale-up and increased column capacity. While commercial agarose resin was employed in this proof-of-concept work, significant improvements in both porosity and surface area for LanM attachment can likely be realized by using other substrates and/or modifications to LanM to increase metal-binding stoichiometry. With respect to scaling, the high expression yield of LanM (80 mg/L with no optimization yet performed) offers promise for the development of a low-cost purification scheme, while the high stability of the LanM column over multiple adsorption/desorption cycles (Figure 2C) supports its reuse potential. A further step critical for scaling will be the conversion from a semicontinuous to a continuous process by employing a rotating column operation that is commonplace in industrial adsorption/desorption operations.[59] In conclusion, while the current LanM-based process should not be considered as a direct competitor for liquid−liquid extraction—particularly with regard to processing concentrated feed solutions from high-grade ore sources—a scaled-up, continuous process would be uniquely positioned to unlock low-grade leachate solutions that are not currently profitable with traditional hydrometallurgical methods.

CONCLUSION

We have demonstrated a reusable, all-aqueous REE extraction and separation platform using an REE-selective protein chelator immobilized on a biorenewable support. This concept represents a crucial step toward sustainable REE production and minimizing global dependence on primary REE resources. Immobilized LanM retained its remarkable REE selectivity and facilitated near-quantitative REE separation from non-REE impurities. Followed by a sequential pH gradient or mild chelator treatment, coextracted Nd/Dy, the most critical REE pair for E-waste recovery, can be separated to high purity (>99.9% purity) within 1 or 2 adsorption/desorption cycles depending on the feed ratio. We further demonstrated the application of LanM for REE extraction and separation into heavy and light REE groups in a single adsorption/desorption cycle, even starting from a highly complex feed solution with low REE content. Our continued efforts are directed at increasing the adsorption capacity to improve productivity, improving selectivity against process impurities, and fine-tuning the REE separation process. However, our process already has several unique advantages over prior art, including its compatibility with low-grade feedstock leachates, its lack of organic solvents, and its ability to achieve high-purity separation of certain critical REEs while using up to ∼90% column capacity. Consequently, this work establishes lanmodulin as the basis for an ecofriendly process for not only REE recovery but also tandem separation that is broadly applicable to both high-grade (e.g., scrap NdFeB magnets) and low-grade (e.g., fly ash) REE feedstocks. Sustainable hydrometallurgical approaches such as the one proposed here will be necessary to implement a coherent transition from the fossil fuel era to low-carbon energies.

ASSOCIATED CONTENT

Supporting Information

The Supporting Information is available free of charge at https://pubs.acs.org/doi/10.1021/acscentsci.1c00724.

Methods including materials, spectrofluorometric titrations of LanM, LanM immobilization and characterization, breakthrough column experiments, inductively coupled plasma mass spectrometry (ICP-MS), and leaching and pH adjustment of PRB coal ash; FT-IR analysis; comparison between the LanM column and reported methods for Nd/Dy separation, and ICP-MS analysis of metal solutions; and additional figures including a characterization of LanM-Cys and column desorption profiles (PDF)

AUTHOR INFORMATION

Corresponding Authors

Joseph A. Cotruvo, Jr. − *Department of Chemistry, The Pennsylvania State University, University Park, Pennsylvania 16802, United States;* orcid.org/0000-0003-4243-8257; Email: juc96@psu.edu

https://doi.org/10.1021/acscentsci.1c00724
ACS Cent. Sci. 2021, 7, 1798−1808

Dan M. Park − *Critical Materials Institute, Physical and Life Sciences Directorate, Lawrence Livermore National Laboratory, Livermore, California 94550, United States;* orcid.org/0000-0002-6000-6805; Email: park36@llnl.gov

Authors

Ziye Dong − *Critical Materials Institute, Physical and Life Sciences Directorate, Lawrence Livermore National Laboratory, Livermore, California 94550, United States;* orcid.org/0000-0002-0419-8523

Joseph A. Mattocks − *Department of Chemistry, The Pennsylvania State University, University Park, Pennsylvania 16802, United States;* orcid.org/0000-0003-1541-0187

Gauthier J.-P. Deblonde − *Critical Materials Institute, Physical and Life Sciences Directorate and Glenn T. Seaborg Institute, Lawrence Livermore National Laboratory, Livermore, California 94550, United States;* orcid.org/0000-0002-0825-8714

Dehong Hu − *Environmental Molecular Sciences Laboratory, Pacific Northwest National Laboratory, Richland, Washington 99354, United States;* orcid.org/0000-0002-3974-2963

Yongqin Jiao − *Critical Materials Institute, Physical and Life Sciences Directorate, Lawrence Livermore National Laboratory, Livermore, California 94550, United States;* orcid.org/0000-0002-6798-5823

Complete contact information is available at: https://pubs.acs.org/10.1021/acscentsci.1c00724

Notes

The authors declare the following competing financial interest(s): Z.D., J.A.M., G.J.-P.D., J.A.C., Y.J., and D.M.P. are listed as inventors on patent applications submitted by Lawrence Livermore National Laboratory and the Pennsylvania State University.

■ ACKNOWLEDGMENTS

We thank Shanwen Wang and Professor Yat Li (University of California Santa Cruz), as well as Dongxiang Wang (Penn State University), for assistance with ICP-MS. We thank Andrew Middleton and Professor Heileen Hsu-Kim (Duke University) for assistance with PRB leaching and ICP-MS. We thank Professor Elizabeth Elacqua (Penn State University) for use of her laboratory's spectrofluorometer. This research is supported by the Critical Materials Institute, an Energy Innovation Hub funded by the U.S. Department of Energy, Office of Energy Efficiency and Renewable Energy, Advanced Manufacturing Office. J.A.C. and J.A.M. also acknowledge support from the U.S. DOE (DE-SC0021007 to J.A.C.). Confocal microscopy was performed in EMSL, a DOE Office of Science User Facility sponsored by the Office of Biological and Environmental Research and located at the Pacific Northwest National Laboratory. This work was performed under the auspices of the U.S. Department of Energy by Lawrence Livermore National Laboratory under Contract DEAC52-07NA27344 (LLNL-JRNL-823707).

■ REFERENCES

(1) Cheisson, T.; Schelter, E. J. Rare earth elements: Mendeleev's bane, modern marvels. *Science* **2019**, *363* (6426), 489.

(2) U.S. Department of Energy. *Critical Materials Strategy*, 2010.

(3) Marx, J.; Schreiber, A.; Zapp, P.; Walachowicz, F. Comparative Life Cycle Assessment of NdFeB Permanent Magnet Production from Different Rare Earth Deposits. *ACS Sustainable Chem. Eng.* **2018**, *6* (5), 5858−5867.

(4) Sprecher, B.; Xiao, Y.; Walton, A.; Speight, J.; Harris, R.; Kleijn, R.; Visser, G.; Kramer, G. J. Life Cycle Inventory of the Production of Rare Earths and the Subsequent Production of NdFeB Rare Earth Permanent Magnets. *Environ. Sci. Technol.* **2014**, *48* (7), 3951−3958.

(5) Wang, L.; Huang, X.; Yu, Y.; Zhao, L.; Wang, C.; Feng, Z.; Cui, D.; Long, Z. Towards cleaner production of rare earth elements from bastnaesite in China. *J. Cleaner Prod.* **2017**, *165*, 231−242.

(6) Xie, F.; Zhang, T. A.; Dreisinger, D.; Doyle, F. A critical review on solvent extraction of rare earths from aqueous solutions. *Miner. Eng.* **2014**, *56*, 10−28.

(7) Vahidi, E.; Zhao, F. Environmental life cycle assessment on the separation of rare earth oxides through solvent extraction. *J. Environ. Manage.* **2017**, *203*, 255−263.

(8) Lee, J. C. K.; Wen, Z. Rare Earths from Mines to Metals: Comparing Environmental Impacts from China's Main Production Pathways. *J. Ind. Ecol.* **2017**, *21* (5), 1277−1290.

(9) Hidayah, N. N.; Abidin, S. Z. The evolution of mineral processing in extraction of rare earth elements using liquid-liquid extraction: A review. *Miner. Eng.* **2018**, *121*, 146−157.

(10) El-Sofany, E. A. Removal of lanthanum and gadolinium from nitrate medium using Aliquat-336 impregnated onto Amberlite XAD-4. *J. Hazard. Mater.* **2008**, *153* (3), 948−954.

(11) Nagaphani Kumar, B.; Radhika, S.; Ramachandra Reddy, B. Solid−liquid extraction of heavy rare-earths from phosphoric acid solutions using Tulsion CH-96 and T-PAR resins. *Chem. Eng. J.* **2010**, *160* (1), 138−144.

(12) Bertelsen, E. R.; Deodhar, G.; Kluherz, K. T.; Davidson, M.; Adams, M. L.; Trewyn, B. G.; Shafer, J. C. Microcolumn lanthanide separation using bis-(2-ethylhexyl) phosphoric acid functionalized ordered mesoporous carbon materials. *J. Chromatogr. A* **2019**, *1595*, 248−256.

(13) Horwitz, E. P.; Chiarizia, R.; Dietz, M. L.; Diamond, H.; Nelson, D. M. Separation and preconcentration of actinides from acidic media by extraction chromatography. *Anal. Chim. Acta* **1993**, *281* (2), 361−372.

(14) Fritz, J. S. Early milestones in the development of ion-exchange chromatography: a personal account. *J. Chromatogr. A* **2004**, *1039* (1), 3−12.

(15) Judge, W. D.; Azimi, G. Recent progress in impurity removal during rare earth element processing: A review. *Hydrometallurgy* **2020**, *196*, 105435.

(16) Ling, L.; Wang, N.-H. L. Ligand-assisted elution chromatography for separation of lanthanides. *J. Chromatogr. A* **2015**, *1389*, 28−38.

(17) Ding, Y.; Harvey, D.; Wang, N.-H. L. Two-zone ligand-assisted displacement chromatography for producing high-purity praseodymium, neodymium, and dysprosium with high yield and high productivity from crude mixtures derived from waste magnets. *Green Chem.* **2020**, *22* (12), 3769−3783.

(18) Florek, J.; Chalifour, F.; Bilodeau, F.; Larivière, D.; Kleitz, F. Nanostructured Hybrid Materials for the Selective Recovery and Enrichment of Rare Earth Elements. *Adv. Funct. Mater.* **2014**, *24* (18), 2668−2676.

(19) Callura, J. C.; Perkins, K. M.; Noack, C. W.; Washburn, N. R.; Dzombak, D. A.; Karamalidis, A. K. Selective adsorption of rare earth elements onto functionalized silica particles. *Green Chem.* **2018**, *20* (7), 1515−1526.

(20) Zhang, H.; McDowell, R. G.; Martin, L. R.; Qiang, Y. Selective Extraction of Heavy and Light Lanthanides from Aqueous Solution by Advanced Magnetic Nanosorbents. *ACS Appl. Mater. Interfaces* **2016**, *8* (14), 9523−9531.

(21) Hu, Y.; Drouin, E.; Larivière, D.; Kleitz, F.; Fontaine, F.-G. Highly Efficient and Selective Recovery of Rare Earth Elements Using Mesoporous Silica Functionalized by Preorganized Chelating Ligands. *ACS Appl. Mater. Interfaces* **2017**, *9* (44), 38584−38593.

(22) Hu, Y.; Misal Castro, L. C.; Drouin, E.; Florek, J.; Kählig, H.; Larivière, D.; Kleitz, F.; Fontaine, F.-G. Size-Selective Separation of Rare Earth Elements Using Functionalized Mesoporous Silica Materials. *ACS Appl. Mater. Interfaces* **2019**, *11* (26), 23681−23691.
(23) Hu, Y.; Florek, J.; Larivière, D.; Fontaine, F.-G.; Kleitz, F. Recent Advances in the Separation of Rare Earth Elements Using Mesoporous Hybrid Materials. *Chem. Rec.* **2018**, *18* (7−8), 1261−1276.
(24) Roca-Sabio, A.; Mato-Iglesias, M.; Esteban-Gómez, D.; Tóth, É.; Blas, A. d.; Platas-Iglesias, C.; Rodríguez-Blas, T. Macrocyclic Receptor Exhibiting Unprecedented Selectivity for Light Lanthanides. *J. Am. Chem. Soc.* **2009**, *131* (9), 3331−3341.
(25) Gupta, N. K.; Gupta, A.; Ramteke, P.; Sahoo, H.; Sengupta, A. Biosorption-a green method for the preconcentration of rare earth elements (REEs) from waste solutions: A review. *J. Mol. Liq.* **2019**, *274*, 148−164.
(26) Mattocks, J. A.; Cotruvo, J. A. Biological, biomolecular, and bio-inspired strategies for detection, extraction, and separations of lanthanides and actinides. *Chem. Soc. Rev.* **2020**, *49* (22), 8315−8334.
(27) Park, D. M.; Reed, D. W.; Yung, M. C.; Eslamimanesh, A.; Lencka, M. M.; Anderko, A.; Fujita, Y.; Riman, R. E.; Navrotsky, A.; Jiao, Y. Q. Bioadsorption of Rare Earth Elements through Cell Surface Display of Lanthanide Binding Tags. *Environ. Sci. Technol.* **2016**, *50* (5), 2735−2742.
(28) Park, D. M.; Brewer, A.; Reed, D. W.; Lammers, L. N.; Jiao, Y. Q. Recovery of Rare Earth Elements from Low-Grade Feedstock Leachates Using Engineered Bacteria. *Environ. Sci. Technol.* **2017**, *51* (22), 13471−13480.
(29) Tay, P. K. R.; Manjula-Basavanna, A.; Joshi, N. S. Repurposing bacterial extracellular matrix for selective and differential abstraction of rare earth elements. *Green Chem.* **2018**, *20* (15), 3512−3520.
(30) Franz, K. J.; Nitz, M.; Imperiali, B. Lanthanide-Binding Tags as Versatile Protein Coexpression Probes. *ChemBioChem* **2003**, *4* (4), 265−271.
(31) Cotruvo, J. A.; Featherston, E. R.; Mattocks, J. A.; Ho, J. V.; Laremore, T. N. Lanmodulin: A Highly Selective Lanthanide-Binding Protein from a Lanthanide-Utilizing Bacterium. *J. Am. Chem. Soc.* **2018**, *140* (44), 15056−15061.
(32) Deblonde, G. J. P.; Mattocks, J. A.; Park, D. M.; Reed, D. W.; Cotruvo, J. A.; Jiao, Y. Selective and Efficient Biomacromolecular Extraction of Rare-Earth Elements using Lanmodulin. *Inorg. Chem.* **2020**, *59* (17), 11855−11867.
(33) Awadhiya, A.; Kumar, D.; Rathore, K.; Fatma, B.; Verma, V. Synthesis and characterization of agarose−bacterial cellulose biodegradable composites. *Polym. Bull.* **2017**, *74* (7), 2887−2903.
(34) Hermanson, G. T. Heterobifunctional Crosslinkers. In *Bioconjugate Techniques*, 3rd ed.; Hermanson, G. T., Ed.; Academic Press: Boston, 2013; Chapter 6, pp 299−339.
(35) Nair, D. P.; Podgórski, M.; Chatani, S.; Gong, T.; Xi, W.; Fenoli, C. R.; Bowman, C. N. The Thiol-Michael Addition Click Reaction: A Powerful and Widely Used Tool in Materials Chemistry. *Chem. Mater.* **2014**, *26* (1), 724−744.
(36) Featherston, E. R.; Issertell, E. J.; Cotruvo, J. A. Probing lanmodulin's lanthanide recognition via sensitized luminescence yields a platform for quantification of terbium in acid mine drainage. *J. Am. Chem. Soc.* **2021**, *143*, 14287−14299.
(37) Baldwin, A. G.; Ivanov, A. S.; Williams, N. J.; Ellis, R. J.; Moyer, B. A.; Bryantsev, V. S.; Shafer, J. C. Outer-Sphere Water Clusters Tune the Lanthanide Selectivity of Diglycolamides. *ACS Cent. Sci.* **2018**, *4* (6), 739−747.
(38) Mattocks, J. A.; Ho, J. V.; Cotruvo, J. A. A Selective, Protein-Based Fluorescent Sensor with Picomolar Affinity for Rare Earth Elements. *J. Am. Chem. Soc.* **2019**, *141* (7), 2857−2861.
(39) Byrne, R. H.; Li, B. Comparative complexation behavior of the rare earths. *Geochim. Cosmochim. Acta* **1995**, *59* (22), 4575−4589.
(40) Hussain, R.; Luo, K. Geochemical Evaluation of Enrichment of Rare-Earth and Critical Elements in Coal Wastes from Jurassic and Permo-Carboniferous Coals in Ordos Basin, China. *Nat. Resour. Res.* **2020**, *29* (3), 1731−1754.
(41) Taggart, R. K.; Hower, J. C.; Dwyer, G. S.; Hsu-Kim, H. Trends in the Rare Earth Element Content of U.S.-Based Coal Combustion Fly Ashes. *Environ. Sci. Technol.* **2016**, *50* (11), 5919−5926.
(42) *Mineral commodity summaries 2020*; Reston, VA, 2020; p 204.
(43) Yang, Y.; Walton, A.; Sheridan, R.; Güth, K.; Gauß, R.; Gutfleisch, O.; Buchert, M.; Steenari, B.-M.; Van Gerven, T.; Jones, P. T.; Binnemans, K. REE Recovery from End-of-Life NdFeB Permanent Magnet Scrap: A Critical Review. *J. Sustainable Metall.* **2017**, *3* (1), 122−149.
(44) Sun, P.-P.; Kim, D.-H.; Cho, S.-Y. Separation of neodymium and dysprosium from nitrate solutions by solvent extraction with Cyanex272. *Miner. Eng.* **2018**, *118*, 9−15.
(45) Yoon, H. S.; Kim, C. J.; Chung, K. W.; Kim, S. D.; Kumar, J. R. Process development for recovery of dysprosium from permanent magnet scraps leach liquor by hydrometallurgical techniques. *Can. Metall. Q.* **2015**, *54* (3), 318−327.
(46) Bogart, J. A.; Lippincott, C. A.; Carroll, P. J.; Schelter, E. J. An Operationally Simple Method for Separating the Rare-Earth Elements Neodymium and Dysprosium. *Angew. Chem., Int. Ed.* **2015**, *54* (28), 8222−8225.
(47) Bogart, J. A.; Cole, B. E.; Boreen, M. A.; Lippincott, C. A.; Manor, B. C.; Carroll, P. J.; Schelter, E. J. Accomplishing simple, solubility-based separations of rare earth elements with complexes bearing size-sensitive molecular apertures. *Proc. Natl. Acad. Sci. U. S. A.* **2016**, *113* (52), 14887−14892.
(48) McGillicuddy, N.; Nesterenko, E. P.; Nesterenko, P. N.; Jones, P.; Paull, B. Chelation ion chromatography of alkaline earth and transition metals a using monolithic silica column with bonded N-hydroxyethyliminodiacetic acid functional groups. *J. Chromatogr. A* **2013**, *1276*, 102−111.
(49) Ashour, R. M.; Samouhos, M.; Polido Legaria, E.; Svärd, M.; Högblom, J.; Forsberg, K.; Palmlöf, M.; Kessler, V. G.; Seisenbaeva, G. A.; Rasmuson, Å. C. DTPA-Functionalized Silica Nano- and Microparticles for Adsorption and Chromatographic Separation of Rare Earth Elements. *ACS Sustainable Chem. Eng.* **2018**, *6* (5), 6889−6900.
(50) Ye, Q.; Li, G.; Deng, B.; Luo, J.; Rao, M.; Peng, Z.; Zhang, Y.; Jiang, T. Solvent extraction behavior of metal ions and selective separation Sc^{3+} in phosphoric acid medium using P204. *Sep. Purif. Technol.* **2019**, *209*, 175−181.
(51) Yagmurlu, B.; Dittrich, C.; Friedrich, B. Effect of Aqueous Media on the Recovery of Scandium by Selective Precipitation. *Metals* **2018**, *8* (5), 314.
(52) Beltrami, D.; Deblonde, G. J. P.; Bélair, S.; Weigel, V. Recovery of yttrium and lanthanides from sulfate solutions with high concentration of iron and low rare earth content. *Hydrometallurgy* **2015**, *157*, 356−362.
(53) Middleton, A.; Park, D. M.; Jiao, Y.; Hsu-Kim, H. Major element composition controls rare earth element solubility during leaching of coal fly ash and coal by-products. *Int. J. Coal Geol.* **2020**, *227*, 103532.
(54) Park, D.; Middleton, A.; Smith, R.; Deblonde, G.; Laudal, D.; Theaker, N.; Hsu-Kim, H.; Jiao, Y. A biosorption-based approach for selective extraction of rare earth elements from coal byproducts. *Sep. Purif. Technol.* **2020**, *241*, 116726.
(55) Smith, R. C.; Taggart, R. K.; Hower, J. C.; Wiesner, M. R.; Hsu-Kim, H. Selective Recovery of Rare Earth Elements from Coal Fly Ash Leachates Using Liquid Membrane Processes. *Environ. Sci. Technol.* **2019**, *53* (8), 4490−4499.
(56) Zhang, N.; Li, H. X.; Liu, X. M. Recovery of scandium from bauxite residue-red mud: a review. *Rare Met.* **2016**, *35* (12), 887−900.
(57) Dong, Z.; Deblonde, G.; Middleton, A.; Hu, D.; Dohnalkova, A.; Kovarik, L.; Qafoku, O.; Shutthanandan, V.; Jin, H.; Hsu-Kim, H.; Theaker, N.; Jiao, Y.; Park, D. Microbe-Encapsulated Silica Gel Biosorbents for Selective Extraction of Scandium from Coal Byproducts. *Environ. Sci. Technol.* **2021**, *55* (9), 6320−6328.
(58) Huang, X.; Dong, J.; Wang, L.; Feng, Z.; Xue, Q.; Meng, X. Selective recovery of rare earth elements from ion-adsorption rare

https://doi.org/10.1021/acscentsci.1c00724
ACS Cent. Sci. 2021, 7, 1798−1808

earth element ores by stepwise extraction with HEH(EHP) and HDEHP. *Green Chem.* **2017**, *19* (5), 1345−1352.
(59) Gabelman, A. Adsorption basics: part 1. *Chemical Engineering Progress* **2017**, *113* (7), 48−53.

https://doi.org/10.1021/acscentsci.1c00724
ACS Cent. Sci. 2021, 7, 1798−1808